

# Surface Profile Description: Invariant Stable Extraction of Straight Line Segments

Patrick Hébert, Denis Laurendeau, and Denis Poussart

Computer Vision and Digital Systems Laboratory  
Department of Electrical Engineering  
Laval University, Québec, Canada  
e-mail: [hebert, laurend, poussart]@gel.ulaval.ca

## Abstract

*This paper presents an approach for the extraction of straight line segments from scattered range measurements on a surface profile. For a given segment, the extracted descriptive parameters should be invariant with the sensor position in the scene and these should also be stable with different measurement sets. While the invariance of the approach is based on a measurement error model which takes into account the sensor's viewpoint, the stability of the result is tested by perturbing the solution. Examples of line extraction are presented for actual measurements acquired with a laser range finder.*

## 1 Introduction

A set of scattered range measurements are collected on a surface from one or multiple viewpoints in the scene and eventually by different sensors. From these measurements, the first operation consists in providing a geometrical description of the visible unknown surface as input to higher level tasks such as pose determination or object recognition. A reliable description may be provided in terms of geometric primitives such as low order polynomial sections [4, 2]. A good description should be compact but more importantly, it should be true to the original surface. In this paper, an approach is proposed to extract straight line segments from data collected on a surface profile.

An important problem that arises in the context of feature extraction is that only a small fraction of points are associated with a straight line segment. The fitting of a primitive should be made robust to outlier data [2, 5, 10, 11]. Outliers are data for which the error distribution appears to depart significantly from the modeled distribution. These may arise from acquisition artifacts or from the presence of other primitives in the scene. Robust techniques have been proposed to overcome the 0% breakdown point associated with standard least-squares methods. Here the breakdown point means the largest percentage of outliers that can be tolerated before the fitted

primitive parameters become arbitrarily distant from the baseline primitive parameters [9]. Point classification is thus necessary since the subsets of the measurements belonging to a unique line segment are not known *a priori*. The interested reader will find a comparative review of the optimization model for extraction and fitting methods in Roth and Levine [9] where standard least-squares, M-estimators, least-median of squares and Hough transform are compared based on their cost functions. Roth and Levine [9] use random sampling to generate an instance of a primitive and then cumulate the number of inliers within a fixed-band around the primitive. A threshold is used to set the fixed-band width and to fix the required number of inliers for a *valid* primitive. Once a valid primitive has been identified, the associated samples are removed. This supposes that the point classification between inliers and outliers is error free. A first question that arises is how to set the fixed-band width and should it be set independently of the viewpoint? Secondly, what is the minimum number of inliers that are required for a valid primitive?

We believe that an acquisition error model should be developed to answer the first question. Since the measurements may be collected from several viewpoints in the scene, the approach must handle errors in both coordinates of the data points in a common referential coordinate system. The error variances may vary between measurement coordinates and among points. Kyriati and Bruckstein [6] define a line fitting cost function that includes a model of error in both coordinates. This cost function allows to make the original Duda and Hart [3] algorithm, based on Hough transform, tolerant to small errors in the coordinates of the data points without giving up its robustness against outliers. They illustrate their idea on simulated data. Even though error variances may vary with the viewpoint, line fitting should not depend on the choice of the referential coordinate system. This will be referred to as the *invariability* of the line fitting.

To answer the second question, we show that an extracted segment is stable if one can detect data redundancy with respect to the primitive model [4]. In this case, a stable segment description is actually supported by a minimal number of inliers; this means that the elimination

or the addition of a measurement should not influence the result. A segment will be valid only if a minimum number of scattered samples have been collected on the same straight line section. In that case, the description is said to be stable for the measurement set.

From the above remarks, we firstly present an acquisition error model that takes the viewpoint into account. The extraction method to identify stable and invariant line segments is presented afterwards.

## 2 View dependent error modeling

Line fitting on noisy data is a regression problem which needs to be independent of the reference frame in which data are collected. Since the reconstructed function of a profile is in  $\mathcal{R}^2$ , noise affects both variables  $x$  and  $z$ . Here we model the uncertainty area of a measurement as an ellipse. The ellipse size and orientation delimit a confidence interval for a measurement. A smaller ellipse is associated with more accurate data and will have more influence on the regression. Uncertainty is modeled as a function of viewpoint. The parameters of the uncertainty ellipses depend on the sensor characteristics, as well as on its position and orientation relative to the object surface. Figure 1 illustrates this line of reasoning. Although measurements are considered independent, measurement error is not identically distributed.

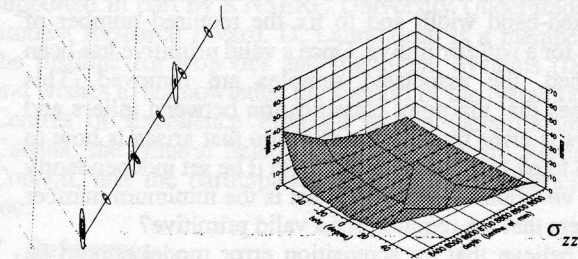


**Figure 1** a) Ellipses of uncertainty on real data: size variation with surface incident angle and depth. b) variance distribution of  $z$ .

The uncertainty model has been developed for but is not restricted to a laser range finder [8]. The error model takes into account the effects of both distance and surface orientation. These two factors act upon the laser energy returned to the sensor. An experiment was conducted to estimate the variance-covariance matrices of  $x$ ,  $z$  values as a function of incident angle and depth. The details of the experiment can be found in Hébert [4]. An uncertainty ellipse is defined by a bidimensional gaussian distribution which approximates the actual distribution. The 99% limits are stored in the model. Extraction of eigenvalues and eigenvectors from each of these covariance matrices allows to define the axes length and orientation of the ellipse relative to the sensor optical axis. The uncertainty model is global. It includes numerical error, as well as depth and incident angle effect. The variance-covariance matrices are

stored in a look-up table where the entries are distance and incident angle. In the studied case, covariance is almost negligible except for large depths or incident angles. In the experiment this happens over 40 degrees for the incident angle and over 800 mm in depth. In figure 1, only the distribution of  $z$  variance is shown.

The gaussian model is valid in the interval of  $\pm 3\sigma$ . Actually, non-gaussian noise sources having an important effect on some small part of the data may exist. For instance, shadow effects generally cause outliers near depth discontinuities. Among other causes of non-gaussian noise, are specular and multiple reflections. This small portion of outliers cannot easily be modeled and they were neglected in the implementation of the noise model.

## 3 Extraction of straight line segments

An error model which takes into account the viewpoint and the distance of the sensor relative to the surface has been defined for invariant fitting. In order to use the noise model, one must know the incident angle between the sensor's optical axis and the surface, as well as the distance  $z$  between the surface and the sensor. However these quantities are in fact what we are looking for. Even if we knew the ellipses of uncertainty associated with every measurement, it would not be possible to apply standard or robust regression techniques since the subsets of the measurements belonging to a unique instance of a line are not known *a priori*. This is part of the extraction problem which does not always lead to a unique solution.

The proposed approach consists in generating an hypothesis for a section and then to verify its validity within the limits of the sensor's noise model. The hypothesis associates a set of measurements to a unique primitive. It is assumed that connectedness has been estimated. This can actually be done in  $O(n \log n)$  [1]. A minimal energy state of the primitive in the parameter space is then searched for in the vicinity of the hypothetical parameters. This is the line fitting stage. The data redundancy with respect to the line model is finally tested by perturbing the minimal energy state of the model and a confidence measure of the stability of the description is computed.

### 3.1 Hypothesis generation: selection of an inlier set

Figure 2 illustrates the hypothesis generation step. In order to generate an hypothesis, a minimal subset is randomly selected among the data points. A minimal subset (MS) is the minimum number of points that are required to uniquely define an instance of a primitive [9]. In the case of a straight line, the MS is composed of two points. The normal parameters  $(\rho_h, \theta_h)$  of the straight line are obtained from the hypothesis. From these parameters, one can access the variance-covariance matrices look-up

table and select an ellipse of uncertainty for every measurements on the profile since the initial hypothesis comprises all points on the profile.

The section is completely defined once its extremities have been identified. In order to find both extreme points of the section, the Mahalanobis distance  $D_{M_i}$  between each point and the straight line is estimated. Every ellipse of index  $i$  is represented in a different rotated reference frame aligned with axes of the ellipse. The expression for  $D_{M_i}$  is simply:

$$D_{M_i} = \frac{1}{\sigma_{x'_i}^2} (X'_i - x'_i)^2 + \frac{1}{\sigma_{z'_i}^2} (Z'_i - z'_i)^2 \quad (1)$$

In this expression,  $(x'_i, z'_i)$  are the coordinates of the  $i^{\text{th}}$  measured point  $P_i$ , expressed in the reference frame defined by the eigenvectors of the corresponding ellipse.  $(X'_i, Z'_i)$  are the coordinates of the point  $P_i'$ , on the straight line for which the distance is estimated.  $\sigma_{x'_i}^2$  and  $\sigma_{z'_i}^2$  are the variances along the ellipse's axes. The set of coordinates  $\{(X'_i, Z'_i)\}$  satisfy the line equation with parameters  $(\rho_h, \theta_h)$  (see Figure 3):

$$\rho = X'_i \cos \theta + Z'_i \sin \theta \quad (2)$$

where  $i = 1, \dots, N$ ,  $\rho = \rho_h$  and  $\theta = \theta_h$

The minimum distance  $D_{M_i}$  between each point and the hypothetical straight line is minimized subject to the constraint that the intersection points  $(X'_i, Z'_i)$  lie on the line defined by  $(\rho_h, \theta_h)$  [6]. We can show that the minimum distance is:

$$D_{M_i} = \frac{(\rho_h - (x'_i \cos \theta'_h + z'_i \sin \theta'_h))^2}{\sigma_{x'_i}^2 \cos^2 \theta'_h + \sigma_{z'_i}^2 \sin^2 \theta'_h} \quad (3)$$

where  $\theta'_h$  is the transformed version of  $\theta_h$  in the point referential. The coordinates of the intersection point on the line are given by the following expressions:

$$Z'_i = \frac{(\sigma_{z'_i}^2 \sin \theta'_h (\rho_h - x'_i \cos \theta'_h) + z'_i \sigma_{x'_i}^2 \cos^2 \theta'_h)}{\sigma_{x'_i}^2 \cos^2 \theta'_h + \sigma_{z'_i}^2 \sin^2 \theta'_h} \quad (4)$$

$$X'_i = \frac{(Z'_i - z'_i) \sigma_{x'_i}^2 \cos \theta'_h}{\sigma_{z'_i}^2 \sin \theta'_h} + x'_i \quad (5)$$

The uncertainty area including 99% of the data has been modeled as a gaussian distribution. Over this limit, that is when  $D_{M_i} \geq 3\sigma$  in  $x'$  and in  $z'$ , data distribution is no more described by the model. The 99% limit defines a maximum size for an ellipse over which a point is classified as an outlier with respect to the hypothesis. Outliers are identified and eliminated from the model point subset.

Since measurements are independent and the connectivity between data points is known, the probability of having two consecutive outliers on a valid section is inferior to  $(0,01)^2$ . Thus we set the section extremities when two consecutive outliers are met. This is illustrated in figure 2.

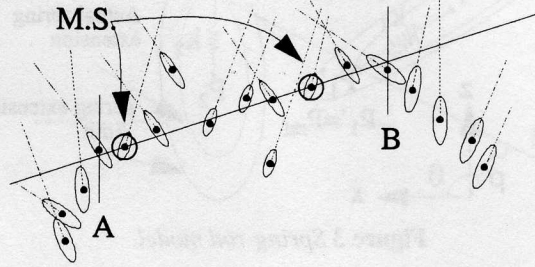


**Figure 2** Generation of a section. A and B are boundaries over which more than 2 consecutive outliers are identified. An outlier is a point whose uncertainty ellipse does not intersect the straight line section.

### 3.2 Equilibrium position: invariant line fitting

At this point, the hypothesis is defined by a MS, the straight line parameters, the section extremities, and the set of inliers within these limits. An ellipse of uncertainty and a distance  $D_{M_i}$  are associated with each inlier. We are now seeking the straight line parameters that minimize the sum of the distance between the inliers and the straight line. To reach this goal, the problem is cast in a minimum energy point identification  $(\rho_e, \theta_e)$  in space  $(\rho, \theta)$  near the hypothetical point  $(\rho_h, \theta_h)$  obtained from the minimal subset. Since the ellipses do not have neither the same size nor the same orientation at each point, a closed-form solution does not exist. An iterative search method is proposed to find the minimum energy state of the straight line model. For this purpose, a spring-rod physical model is defined as illustrated in figure 3. Springs are anchored to data points  $P_i$  and initially attached to the rod at the estimated intersection points  $P_i'$  computed with equations (4) and (5).

The pulling force in a spring is equal to the Mahalanobis distance  $D_{M_i}$ . The spring constant  $k_i$  is estimated at one iteration from the ratio of the force over the Euclidean distance between  $P_i$  and  $P_i'$ . That estimate is updated after every iteration. Attach points  $P_i'$  are fixed for a given iteration. The equilibrium position is computed by solving the following system of equations over the inliers.

$$\sum_i F_{x_i} = \sum_i F_{z_i} = \sum_i \tau_{x_i} = \sum_i \tau_{z_i} = 0 \quad (6)$$

The resulting system, including force ( $F$ ) and torque ( $\tau$ ) components, allows to compute the equilibrium straight line parameters. Since the constants are estimated and the attach points are also estimated, the ellipses, the attach points, and the force are recomputed iteratively. Moreover,

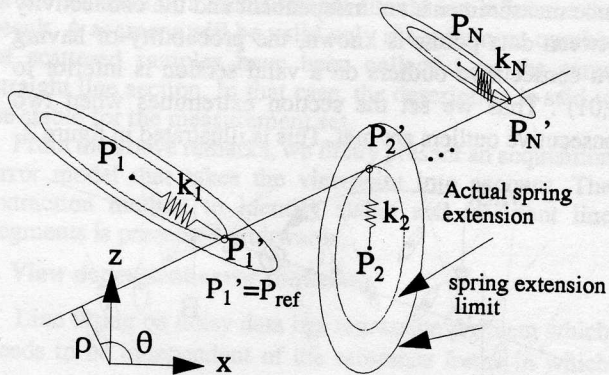


Figure 3 Spring-rod model.

since the section is allowed to move in 2-D space, the section boundaries and the inliers set are re-evaluated following each iteration. The equilibrium position is reached when the system of equations (6) is verified at the beginning of an iteration.

### 3.3 Stability test of a section: perturbation

A plausible hypothesis has been generated from two points randomly sampled on the profile. A minimum of energy was also found in the space of parameters  $(\rho_e, \theta_e)$  of the straight line description. What can be said about the stability of this solution? When one perturbs the system, does the computed local minimum remain the same or does it migrate towards another local minimum? In that case, the extracted primitive would be sensitive to the set of measurements sampled on the object surface. We want to know whether that set of measurements supports the hypothesis or not; that is *is there redundancy in the measurements relative to the line model?*

The system is perturbed if one removes temporarily the two points of the MS and then re-evaluates the equilibrium state of the section. The equilibrium state should move. The two removed points are then re-inserted and the equilibrium state is recomputed. If the rod returns to its original position, we say that the section is stable. A perturbation can cause a spring to break; this means that a measurement becomes an outlier. In that case, this also means that the solution has moved towards another local minimum. The stability test is illustrated in figure 4.

Since the total number of points is finite, the number of local minima is also finite. In practice, many hypotheses are explored concurrently on the whole signal. Moreover, the rapidity of the search process can be improved if the random samples of the MS are constrained to lie in a given neighborhood. This approach shares similarities with conventional stochastic optimization approaches such as simulated annealing but with the difference that the perturbation is caused by the energy function deformation instead of temperature control.

### Algorithm

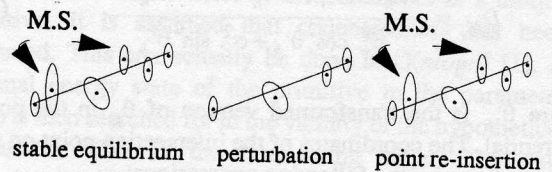
- ```

/* hypothesis generation */
- Select an M.S. by random sampling
- Compute the corresponding parameters  $(\rho_h, \theta_h)$ 

/* equilibrium position */
While the equilibrium state is not reached
- Select uncertainty parameters for every
  points with noise model and hypothetical
  parameters
- Compute line extremities
- Evaluate spring constants and forces
- Identify outlier points within the line section
- Compute the new line parameters that mini-
  mize the system energy

/* perturbation */
- Remove the M.S.
- Compute the equilibrium position
- Re-insert the M.S.
- Compute the equilibrium position
- if the line returns to its original equilibrium position
  - Tag the section as stable
- else
  - Reject the hypothesis
  
```

#### Case of a stable segment



#### Case of an instable segment



Figure 4 Stability test on a segment.

### 4 Results

For every stable section, the measurements, the extremities, the ellipses of uncertainty, the intersection points and outlier measurements are included in a list structure. The quality of a section is characterized by a validity index which is defined as the number of valid

measurements (inliers) and the ratio of the variance of the section's inlier coordinates estimated in a reference frame aligned with the stable equilibrium state line description. This ratio provides a comparison between the variance explained by the model and the residual error.

The complete list includes all identified sections. Two extracted sections can overlap partially or completely. In the full version of the list, no solution is discarded. With task-dependent requirements on precision, the original data can be compressed to keep only a minimum set of sections and points that are not associated to any section. The latter points lie on areas where more data must be acquired to reconstruct the profile or areas that cannot be modeled adequately by straight line description.

The proposed method was implemented and tested on machine made objects. Figure 5 shows the effect of density variation in measurements. The actual object is composed of straight line sections. In (a), the profile is acquired from a single viewpoint. The extracted stable segments are superimposed on data points as dark lines. In (b) the profile is acquired from three different viewpoints and the sampling density is locally increased. In (c) the measurement density was slightly increased; one can easily see that the measurements are not regularly distributed on the profile. In (d), the laser rays and the stable segments are superimposed. We can observe the appearance of stable line segments on top of the object and on the right side. Figure 5(e) clearly shows the 99% uncertainty ellipse size variation with surface incident angle. One can also observe the intersection point between the ellipse and the segment.

The example in figure 6 illustrates the multiplicity of solutions in segmentation. Three lines are almost identical and correspond to three close local minimum in parameter space. The slight difference between these lines is explained by different inlier sets which arise from different initial minimal subsets. In the figure, the ellipses are drawn for a single solution.

In figure 7, the actual object is composed of straight line and circular sections. Figure 7(b) illustrates two outliers that originate from shadow effects. In figure 7(c), a straight line was detected on an actual circular arc. With this particular sample set composed of four inliers and within the precision limits of the sensor, the stability hypothesis cannot be rejected.

## 5 Conclusion

The descriptions are obtained where there exists redundancy in the signal with respect to the line model. Redundancy identification is performed in the extraction process by a perturbation strategy. Moreover, the data uncertainty model ensures the invariability of the fitting relative to sensor position. It also includes all tolerance parameters and allows for the elimination of arbitrary

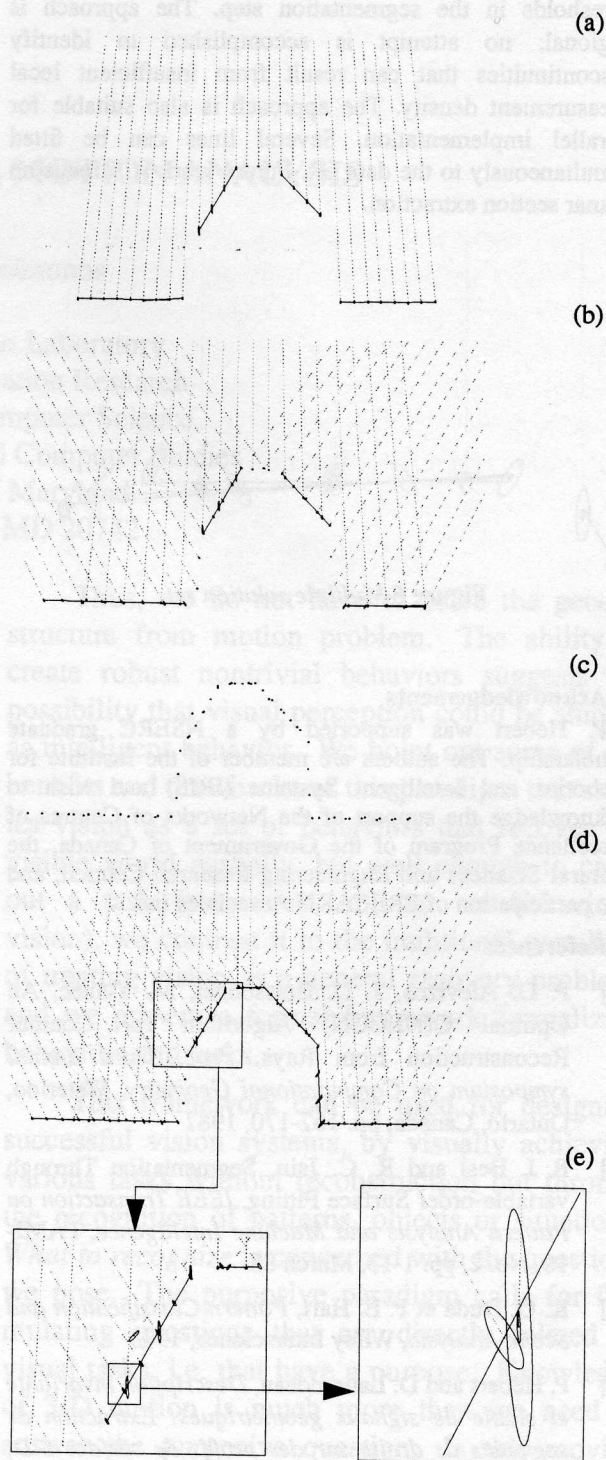


**Figure 5** (a) (b) and (d) Effect of density measurement variation on segment extraction. (c) illustration of the measurement distribution on profile (d). (e) zoom on ellipses of uncertainty (99%) and intersection point on segment.

thresholds in the segmentation step. The approach is regional; no attempt is accomplished to identify discontinuities that can result from insufficient local measurement density. The approach is also suitable for parallel implementation. Several lines can be fitted simultaneously to the data set. Future work will focus on planar section extraction.

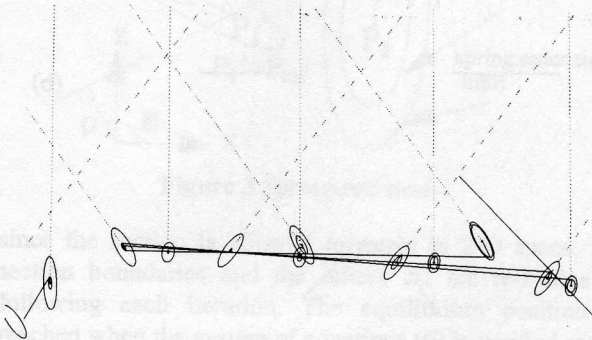


Figure 6 Multiple solution set.

## 6 Acknowledgements

P. Hébert was supported by a NSERC graduate scholarship. The authors are member of the Institute for Robotics and Intelligent Systems (IRIS) and wish to acknowledge the support of the Networks of Centres of Excellence Program of the Government of Canada, the Natural Sciences and Engineering Research Council, and the participation of PRECARN Associates Inc.

## 7 References

- [1] P. D. Alevizos, J. D. Boissonnat, M. Yvinec, An Optimal  $O(N \log N)$  Algorithm for Contour Reconstruction from Rays, *Proc. Third annual symposium on Computational Geometry*, Waterloo, Ontario, Canada, pp. 162-170, 1987
- [2] P. J. Besl and R. C. Jain, Segmentation Through variable-order Surface Fitting, *IEEE Transaction on Pattern Analysis and Machine Intelligence*, PAMI-10, No. 2, pp. 1-13, March 88
- [3] R. O. Duda et P. E. Hart, *Pattern Classification and Scene Analysis*, Wiley Interscience, 1973
- [4] P. Hébert and D. Laurendeau, *Description invariante et stable de signaux géométriques: Extraction de segments de droite sur des profils de surface 3-D*, Technical Report RT-VSN-92-10, VSN Lab, Dept. of EE, Laval University, Ste-Foy, Québec, Canada, Oct. 1992
- [5] B. Kamgar-Parsi, B. Kamgar-Parsi, and N. S. Netanyahu, A Nonparametric Method for Fitting a Straight Line to a Noisy Image, *IEEE Transaction on Pattern Analysis and Machine Intelligence*, PAMI-

11, No 9, pp. 998-1001, April 1992

- [6] N. Kiryati and A. M. Bruckstein, What's in a Set of Points?, *IEEE Transaction on Pattern Analysis and Machine Intelligence*, PAMI-14, No 4, pp. 496-500, April 1992
- [7] P. Lancaster and K. Salkauskas, *Curve and Surface Fitting*, Academic, London, 1986
- [8] M. Rioux, Laser Range Finder Based on Synchronized Scanners, *Applied Optics*, vol. 23, no. 21, pp. 3837-3844, Nov. 1984
- [9] G. Roth and M. D. Levine, *Extracting Geometric Primitives*, Technical report TR-CIM-92-13, McGill Research Centre for Intelligent Machines, McGill University, Montréal, Québec, Canada, Oct. 1992
- [10] A. Stein and M. Werman, Robust Statistics in Shape Fitting, *Proc. of the IEEE Conf. on Computer Vision and Pattern Recognition*, Champaign, Illinois, USA, pp. 540-546, 1992
- [11] I. Weiss, Line Fitting in a Noisy Image, *IEEE Transaction on Pattern Analysis and Machine Intelligence*, PAMI-11, No. 3, pp. 325-329, March 89

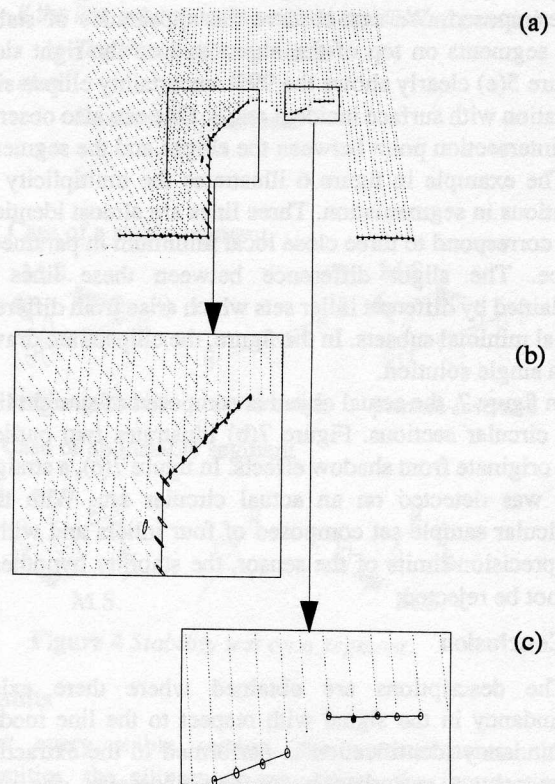


Figure 7 Actual segmentation on a composite profile of straight lines and conical sections.